



ELSEVIER

Biochimica et Biophysica Acta 1430 (1999) 25–38

BIOCHIMICA ET BIOPHYSICA ACTA

**BBA**

## Structural and kinetic properties of adenylyl sulfate reductase from *Catharanthus roseus* cell cultures

Antje Prior<sup>a</sup>, Joachim F. Uhrig<sup>1,a</sup>, Lisa Heins<sup>b</sup>, Annette Wiesmann<sup>a</sup>,  
Christopher H. Lillig<sup>a</sup>, Corinna Stoltze<sup>a</sup>, Jürgen Soll<sup>b</sup>, Jens D. Schwenn<sup>a,\*</sup>

<sup>a</sup> Lehrstuhl Biochemie der Pflanzen, Ruhr-Universität-Bochum, Bochum ND 2-149, 44780 Bochum, Germany

<sup>b</sup> Botanisches Institut der Christian-Albrechts-Universität zu Kiel, Kiel, Germany

Received 22 July 1998; received in revised form 28 October 1998; accepted 24 November 1998

### Abstract

A cDNA encoding a plant-type APS reductase was isolated from an axenic cell suspension culture of *Catharanthus roseus* (Genbank/EMBL-databank accession number U63784). The open reading frame of 1392 bp (termed *par*) encoded for a protein ( $M_r = 51394$ ) consisting of a N-terminal transit peptide, a PAPS reductase-like core and a C-terminal extension with homology to the thioredoxin-like domain of protein disulfide isomerase. The APS reductase precursor was imported into pea chloroplasts in vitro and processed to give a mature protein of  $\approx 45$  kDa. The homologous protein from pea chloroplast stroma was detected using anti:*par* polyclonal antibodies. To investigate the catalytical function of the different domains deleted *par* proteins were purified. *Par* $\Delta 1$  lacking the transit sequence liberated sulfite from APS ( $K_m 2.5 \pm 0.23 \mu\text{M}$ ) in vitro with glutathione ( $K_m 3 \pm 0.64 \text{ mM}$ ) as reductant ( $V_{\text{max}} 2.6 \pm 0.14 \text{ U mg}^{-1}$ , molecular activity  $126 \text{ min}^{-1}$ ). *Par* $\Delta 2$  lacking the transit sequence and C-terminal domain had to be reconstituted with exogenous thioredoxin as reductant ( $K_m 15.3 \pm 1.27 \mu\text{M}$ ,  $V_{\text{max}} 0.6 \pm 0.014 \text{ U mg}^{-1}$ ). Glutaredoxin, GSH or DTT were ineffective substitutes. *Par* $\Delta 1$  (35.4%) and *par* $\Delta 2$  (21.8%) both exhibited insulin reductase activity comparable to thioredoxin (100%). Protein disulfide isomerase activity was observed for *par* $\Delta 1$ . © 1999 Elsevier Science B.V. All rights reserved.

**Keywords:** Sulfate assimilation; Plant adenylyl sulfate reductase; Chloroplast; Protein disulfide isomerase; Thioredoxin; Cell culture

### 1. Introduction

To support the biosynthesis of cysteine and methionine with the element S, plants, like most other prototrophic organisms, reduce inorganic sulfate to sulfide. The reduction of inorganic sulfate is a multi-step process in which the relatively inert sulfate is activated to give an adenylylated form in the first phase. In the second phase, the activated sulfate is reduced successively to sulfite and sulfide. The sulfide sulfur is then incorporated into *O*-acetyl-L-serine yielding cysteine. The enzymatic mechanism of sulfite formation in plants is not completely understood. In

Abbreviations: *A*, absorbance; AMP, adenosine 5'-monophosphate; APS, adenylyl sulfate; CMP, cytidine monophosphate; DCPIP, dichlorophenol indophenol; DTT, dithiothreitol; grx, glutaredoxin; GSH, reduced glutathione; GSSG, oxidized glutathione; PAP, adenosine 3',5'-diphosphate; PAPS, 3'-phosphoadenylyl sulfate; SDS-PAGE, sodium dodecylsulfate polyacrylamide gel electrophoresis; trx, thioredoxin

\* Corresponding author. Fax: +49 (234) 709-4396;

E-mail: jens-dirk.h.schwenn@rz.ruhr-uni-bochum.de

<sup>1</sup> Present address: Max Planck Institut für Züchtungsfor-schung, Köln.

the current discussion a plant type APS reductase<sup>2</sup> is proposed to catalyze the reduction of adenyly sulfate to sulfite with a thiol as reductant [1,2]. In the older literature, a similar reaction was described as APS sulfotransferase reaction. This enzyme was proposed to produce a bound sulfite by transferring the sulfate from APS to a sulfite carrier molecule [3,4]. A third possibility of sulfite formation that exists in bacteria and lower eukaryotes, where PAPS instead of APS is reduced by a PAPS reductase to free sulfite has also been discussed to occur in higher plants [5]. The PAPS reductase mechanism that relies on thioredoxin or glutaredoxin as reductant has been investigated in more detail in *Escherichia coli*. Steady-state kinetics [6] and a high resolution 3-dimensional structure of the enzyme protein [7] provided a good basis to understand and clarify the reaction mechanism. As yet, the mechanism of sulfite formation in higher plants has not reached this point. The great instability of enzymes and the high reactivity of reduced or activated sulfur compounds, as well as inadequately defined reactions and reaction conditions have frequently obscured the nature of reactions that are involved in the reduction of sulfate to sulfite in plants. Moreover, the low intracellular concentrations of the enzymes participating in this reduction has been just another obstacle in the study of their catalytic properties. Recombinant proteins nowadays provide invaluable tools for the study of enzymes participating in the assimilation of sulfate and the biosynthesis of cysteine and glutathione. Most of the earlier biochemical work on plant sulfate reduction [8] is now supported by molecular data characterizing genes and gene products involved in this pathway [9]. Many of the gene products from plant cDNAs are structurally quite similar to the corresponding bacterial and fungal proteins [10–12] indi-

---

<sup>2</sup> It has been termed APS reductase in accordance with the proteins detected recently in *Arabidopsis thaliana*, but it has no structural or functional similarity with the better known APS reductase (EC 1.8.99.4) found in anaerobic sulfate reducers, phototrophic purple and green sulfur bacteria and chemotrophic species of the archaeo- and eubacteria. The plant-type APS reductase described here does not contain flavins or iron sulfur clusters. While bacterial APS reductases catalyze an easily reversible reaction, the name APS reductase is used for par gene product from *C. roseus* only to indicate its capability to reduce APS to sulfite and AMP.

cating a common evolutionary origin. But despite these homologies between plant enzymes and their microbial counterparts, the higher morphological differentiation of the plant cell and its highly differentiated cellular compartmentation demand for specific isoforms. As a consequence, any molecular approach to study the cysteine pathway in correlation with the gene activity by monitoring the content of mRNA from whole plants or parts of the plant has to take into account that, in addition to the experimental parameters, a complex pattern of spatial and developmental factors affect or even obscure the response. In order to minimize these imponderables, we started to investigate dedifferentiated cloned plant cells from *Catharanthus roseus* L.G. Don [13] as a source of morphologically and physiologically homogeneous, isogenic plant material. We have shown earlier that these cells can grow on sulfate [14,15] and equally well on methionine [16] as a single source of sulfur. In comparison to whole plants, nutrients can be applied directly to the medium and structures or mechanisms of the vascular transport can be neglected. This may be advantageous in the study of a cellular response to nutritional stress [17] which is besides heavy metal poisoning the most widely applied tool to induce sulfate metabolizing enzymes.

In this work, we present structural and biochemical properties of a recombinant plant APS reductase expressed from a cDNA isolated from *C. roseus* cell suspension culture. With emphasis on its structural properties, the kinetic constants of the recombinant protein were determined applying steady-state kinetics. Using a coupled in vitro transcription and translation assay we investigated the import and processing of the precursor protein into intact chloroplasts. In addition, first evidence is presented for the occurrence of an immunologically related endogenous APS reductase in chloroplast stroma from *Pisum sativum*.

## 2. Materials and methods

### 2.1. Bacterial strains

*E. coli* XL1 Blue MRF':  $\Delta(mcrA)183$ ,  $\Delta(mcrCB-hsdSMR-mrr)173$ , *endA1*, *supE44*, *thi-1*, *recA1*, *gyrA96*, *relA1*, *lac* [F', *proAB*, *lacI*<sup>q</sup> Z $\Delta$ M15,

Tn10(Tet<sup>r</sup>). *E. coli* SOLR: e14<sup>-</sup>(McrA<sup>-</sup>),  $\Delta$ (*merCB-hsdSMR-mrr*)171, *sbcC*, *recB*, *recJ*, *uvrC*, *umuC*::Tn5 (Kan<sup>r</sup>), *lac*, *gyrA96*, *relA1*, *thi-1*, *endA1*,  $\lambda^+$ , [F', *proAB*, *lacI<sup>q</sup>*, Z $\Delta$ M15]<sup>c</sup>, Su<sup>-</sup>, (non-suppressing) (Stratagene). *E. coli* JM96 FAK: *thr-1*, *leuB6*, *trp-1*, *hisG1*, *cysH56*, *argH1*, *thi-1*, *ara13*, *lacY1*, *gal-6*, *malA1*, *xyl-7*, *mtl-2*, *strA9*, *tonA2*,  $\lambda^+$ ,  $\lambda^-$ , *supE44*, *hsdR2* by P1 transduction of Zjj-202::tn10(Tet<sup>r</sup>) [18]. *E. coli* BL21(DE3): F', *ompT*, *hsdS<sub>B</sub>* (r<sub>B</sub><sup>-</sup>r<sub>M</sub><sup>-</sup>), *gal*, *dcm* (DE3) [19] (Novagen).

## 2.2. Plasmids and oligonucleotides

Plasmids pCR*par2* and pCR*par4* containing the EcoRI/XhoI cloned *par*-cDNA were isolated from a *C. roseus* pBluescript-II-SK<sup>-</sup>-cDNA library by complementing the *E. coli* mutant JM96 FAK. pCR*par4* contained the full-length *par*-cDNA, whereas pCR*par2* represented a truncated cDNA starting from amino acid 71. pET16b (Novagen) derivative pET16b*par* $\Delta$ 1 harboring the deleted *par*-cDNA as BamHI/BglII fragment from pCR*par2* was used for expression of recombinant *par* protein as his<sub>10</sub>-fusion without transit peptide (*par* $\Delta$ 1). pET16*par* $\Delta$ 2 contains the 764 bp BamHI-PCR-fragment from pCR*par4* using the oligonucleotides PR*par*Met1 (5'-CACACAGGATCCAATGCCCGAGGTTGAGAGAAAGTTG-3') and PR*par*Del (5'-CACACAGGATCCCCCTTTGTGTAAACCCACAT-3') and was used for expression of the N- and C-terminal deleted protein *par* $\Delta$ 2.

## 2.3. Growth of bacteria, transformation and selection

Bacteria were grown on Vogel–Bonner as minimal medium [20] otherwise LB broth was used [21]. *E. coli* JM96 FAK was used for complementation and was supplemented with a mixture of amino acids (Trp, His, Arg, Leu and Thr at 1 mM each), 100 mg l<sup>-1</sup> ampicillin, 10 mg l<sup>-1</sup> tetracycline and 10  $\mu$ M thiamine. Bacterial transformation was performed according to [22] or by electroporation [23] with the 'Gene Pulser' (Bio-Rad).

## 2.4. Growth of *Catharanthus roseus* suspension cultures

*C. roseus* cells were grown heterotrophically ac-

cording to [13] in LS medium [24]. For growth in sulfate-deficient medium, LS was modified by replacing the sulfate by equimolar amounts of the corresponding nitrate salts. After growth for 5 days in LS medium, the cells were harvested, washed twice with sulfate-free medium and then transferred to the sulfate-deficient medium.

## 2.5. RNA isolation and cDNA synthesis

Washed *C. roseus* cells were dried on a Büchner funnel, resuspended in GTC buffer (4 M guanidine-isothiocyanate, 25 mM Na-citrate pH 7.0, 0.5% *N*-laurylsarcosine, 100 mM  $\beta$ -mercaptoethanol) and disrupted by two passages through a French press (Sorvall Ribi Cell Fractionator) with 14.2 MPa at 5°C. The isolation of total RNA from this homogenate was carried out according to [25] by acid phenol extraction and a subsequent CsCl gradient centrifugation. The RNA was stored in 70% ethanol at -80°C. Poly-A<sup>+</sup>-mRNA was isolated from total RNA with Oligotex-d(T) (Qiagen) according to the manufacturer's instructions. The cDNA library was constructed from 5  $\mu$ g poly-A<sup>+</sup>-mRNA using the  $\lambda$ -Zap-cDNA Synthesis Kit and packaging into phage particles with the Gigapack II Gold Kit (Stratagene). Phages were propagated in *E. coli* XL1 Blue MRF'. The plasmid-library in pBluescript-II-SK<sup>-</sup> was prepared by in vivo excision from a  $\lambda$ -Zap-II-cDNA library according to [26].

## 2.6. General methods

Principal methods used for isolation, restriction and cloning of DNA, agarose gel electrophoresis and PCR were performed according to [21]. DNA sequencing was done with an automated DNA-Sequencer using the Auto Read Sequencing Kit (Pharmacia) with fluorescein-labeled primers. Annealing temperatures for oligonucleotides were calculated depending on their G:C content and the inserted mismatches. The concentration of protein was determined colorimetrically using Coomassie brilliant blue R 250 [27]. SDS-PAGE was run on 12.5% gels as described by [28]. Polyclonal anti:*par* or anti:PAPS reductase antibodies from rabbit were used to detect the *par* gene products by Western immunoblotting [29]. Immunoprecipitates were visualized on

nitrocellulose BA-S 85 (Schleicher and Schuell) by peroxidase-conjugated goat:anti-rabbit immunoglobulins or, for higher sensitivity, with alkaline phosphatase-conjugated goat:anti-rabbit immunoglobulins. 4-Chloro-1-naphthol in methanol or Fast red TR/naphthol AS-MX were used for detection.

## 2.7. Protein expression, extraction and purification

For recombinant expression of the *parΔ1* or *parΔ2* protein *E. coli* BL21(DE3) was transformed with the plasmids pET16*parΔ1* or pET16*parΔ2*. Transformants were grown in LB medium containing 100 mg l<sup>-1</sup> ampicillin. At A<sub>595</sub> 0.6 expression of the fusion protein was induced by adding 0.5 mM isopropyl-β-D-thiogalactoside (IPTG). The cells were harvested after another 3 h, resuspended in 20 mM Tris/HCl buffer with 100 mM NaCl and ruptured by using a French press (Sorvall Ribi Cell Fractionator). Expressed his<sub>10</sub>-tag proteins were purified from the crude extract using the TALON metal affinity resin (Clontech) following the instructions of the manufacturer. His<sub>10</sub>-tag proteins were eluted with the above described Tris buffer including 200 mM imidazole. Expression of *cysH* gene and purification of *E. coli* PAPS reductase was performed as described in [6]. For expression of CR*par4* cDNA in *E. coli* JM96FAK the culture was grown overnight in Vogel–Bonner minimal medium.

## 2.8. Enzyme assays

### 2.8.1. APS reductase assay

APS reductase activity was assayed by measuring acid-volatile [<sup>35</sup>S]sulfite formed from [<sup>35</sup>S]APS as described by [30]. The assay mixture (100 μl) contained 1–100 ng of purified his<sub>10</sub>-tag *par* protein, 100 mM Tris/HCl pH 8.0, 10 mM Na<sub>2</sub>SO<sub>3</sub>, 0.5 M Na<sub>2</sub>SO<sub>4</sub>, 2–15 μM [<sup>35</sup>S]APS (specific radioactivity, 1.7 kBq nmol<sup>-1</sup>), 50 μM–20 mM DTT or GSH and for the *parΔ2* protein additionally 2–50 μM *E. coli* thioredoxin-1 (MBI Fermentas) or glutaredoxin-1. [<sup>35</sup>S]PAPS was prepared enzymatically from [<sup>35</sup>S]SO<sub>4</sub><sup>2-</sup> (Amersham-Buchler) according to [31] in a reaction system containing recombinant his<sub>10</sub>-tag APS kinase from *A. thaliana* [32] and auxiliary enzymes (ATP sulfurylase and inorganic pyrophosphatase from Sigma, pyruvate kinase and phosphoenol-

pyruvate from Boehringer, Mannheim). [<sup>35</sup>S]APS was produced by dephosphorylating 530 nmol [<sup>35</sup>S]PAPS with 20 units P1 nuclease from *Penicillium citrinum* (Boehringer, Mannheim) incubating for 30 min at 30°C. PAPS synthesis or conversion of PAPS to APS was monitored by HPLC as described earlier [33].

### 2.8.2. Assay of insulin disulfide reduction

The preparation of insulin stock solution and the reduction of insulin disulfide was done according to [34]. The protein to be tested was incubated on ice for 5 min with 5 mM DTT in a volume of 100 μl. The assay was started by mixing 500 μl freshly diluted insulin solution (1 mg ml<sup>-1</sup> in 0.1 M potassium phosphate pH 7.0, 2 mM EDTA) with the preincubated reduced protein. The final reaction mixture contained DTT, *trx1* from *E. coli*, *parΔ1*, *parΔ2* or *E. coli* PAPS reductase as indicated.

### 2.8.3. Reactivation of reduced and denatured RNase

Reduced, denatured RNase A was prepared as described in [35]. For reactivation of reduced RNase, the enzyme was treated with *parΔ1* protein or *E. coli* PAPS reductase as indicated at a final concentration of 0.07 mg ml<sup>-1</sup> in redox buffer (0.2 mM DTT, 0.3 mM GSSG, 3.3 mM MgCl<sub>2</sub>, 15 mM Tris/acetate pH 8.0). At appropriate intervals 80-μl portions were withdrawn from the reactivation assay and mixed with 1.12 ml of cyclic 2',3'-CMP (0.8 mg ml<sup>-1</sup> in Tris/HCl pH 7.4) and incubated for 5 min [36]. Hydrolysis of cyclic 2',3'-CMP was measured by the increase of absorbance at 296 nm [37].

### 2.8.4. Measurement of diaphorase activity

Diaphorase activity was tested colorimetrically monitoring the bleaching of DCPIP at 600 nm. The assay contained 83.3 mM potassium phosphate pH 5.9, 0.05 mM EDTA, 1.53 mM DCPIP, 0.67 mg ml<sup>-1</sup> bovine albumin, 0.2 mM NADH and up to 1.15 μM *parΔ1*, *parΔ2* or 12.4 nM diaphorase from pig heart.

## 2.9. In vitro translation, chloroplast import and preparation of chloroplast fractions

For in vitro transcription plasmid pCR*par4* was

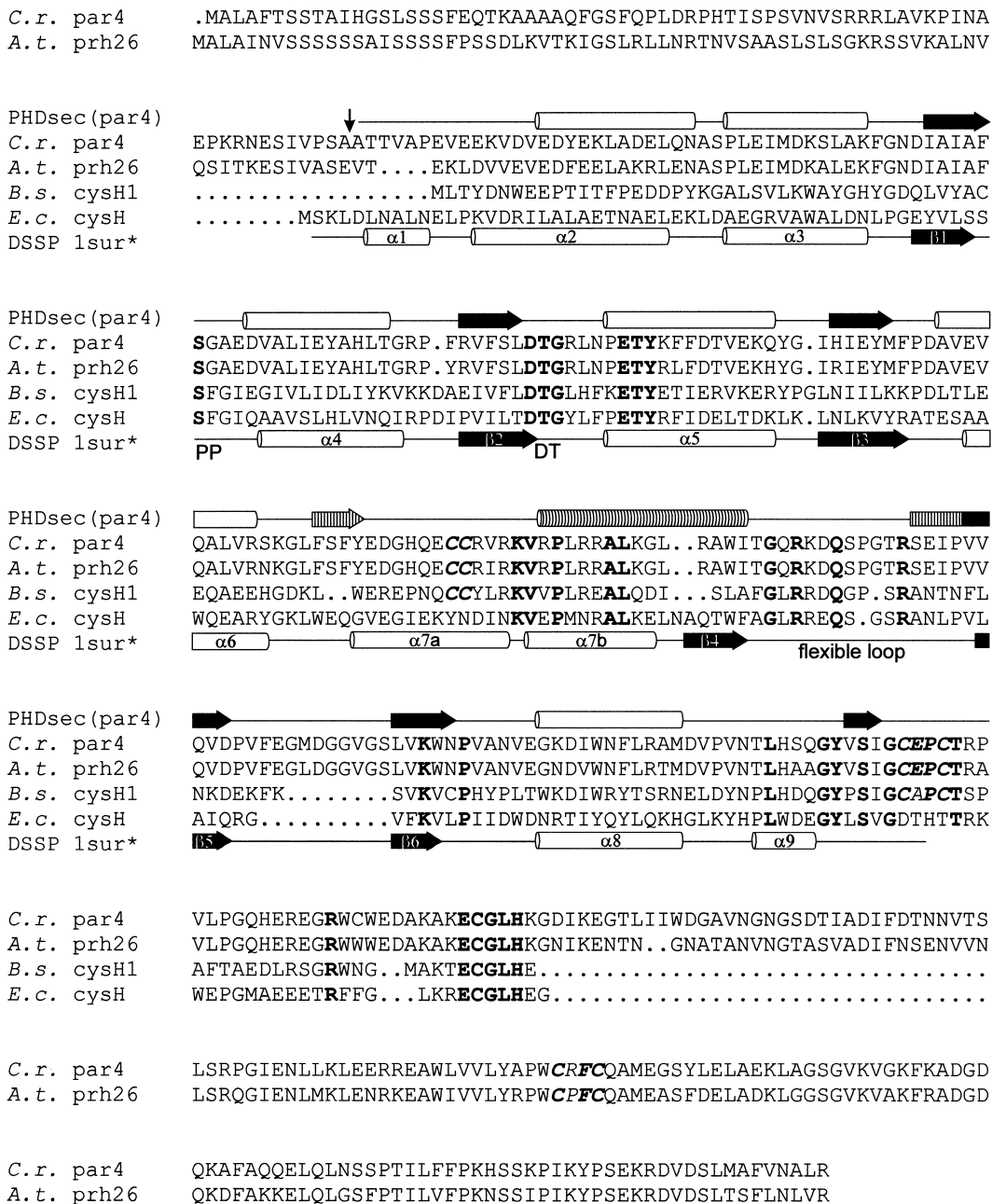


Fig. 1. Multiple sequence alignment and secondary structure prediction for the CRpar4 protein. Comparison of the *Catharanthus roseus* par protein (*C. r. par4*; accession number: U63784), the *Arabidopsis thaliana* prh26 protein (*A. t. prh26*; U53865) [1], the *cysH* homolog from *Bacillus subtilis* (*B. s. cysH1*; U76751) [41], and *E. coli* PAPS reductase (*E. c. cysH*; P17854) [18]. Conserved residues are printed in bold, the cysteine motifs in bold and italic letters. The vertical arrow marks the putative cleavage site for the transit peptide. The secondary structure prediction for the *C. r. par4* protein (PHDsec) was done according to [47–49]. Secondary structure assignment for *E. coli* PAPS reductase (protein data bank accession number: 1sur) was done with DSSP [59] (DSSP 1sur). The designation of secondary structure elements is given according to [7]. The modified PP motif (PP), the DT motif, and the flexible loop are marked according to [7,46]. \*1sur is on hold until April 1st, 1999.

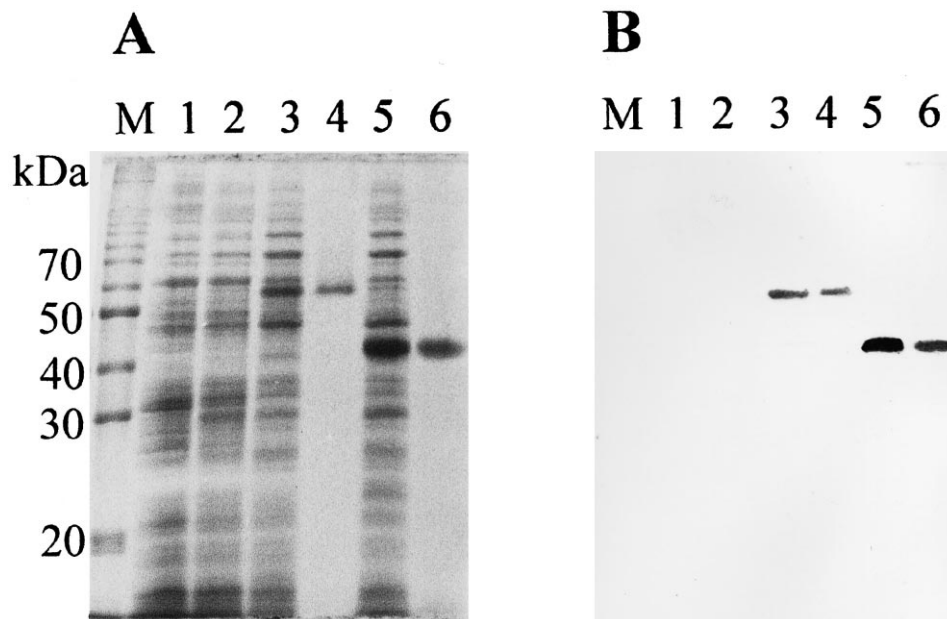


Fig. 2. Expression and purification of *parΔ1* and *parΔ2*. (A) SDS-PAGE (12.5%, Coomassie blue staining) and (B) Western blot showing the *parΔ1* and *parΔ2* gene products as *his*<sub>10</sub>-tag fusion expressed in *E. coli* BL21(DE3). Immunodetection of the recombinant *par* gene products was performed using the anti-*parΔ1* antibody and peroxidase conjugated goat:anti-rabbit immunoglobulins. Lanes: M, molecular weight marker (10 kDa ladder, MBI Fermentas); 1, crude protein extract of *E. coli* BL21(DE3) (12 μg); 2, crude protein extract of *E. coli* BL21(DE3) transformed with vector pET16b (12 μg); 3, crude protein extract of *E. coli* BL21(DE3) transformed with pET16*parΔ1* (12 μg); 4, purified *parΔ1* protein (1 μg); 5, crude protein extract of *E. coli* BL21(DE3) transformed with pET16-*parΔ2* (12 μg); 6, purified *parΔ2* protein (2 μg).

linearized with endonuclease *XhoI* and transcription was carried out for 2 h at 37°C using T3 RNA-polymerase (MBI, Fermentas) [38]. The subsequent *in vitro* translation was done in reticulocyte lysate (Amersham-Buchler) without magnesium acetate according to [39]. Preparation of chloroplasts and chloroplast import was carried out as published in [40]. Departing from this protocol, chloroplasts equivalent to 50 μg chlorophyll were used in 100 μl import mix. Prebinding of precursor protein to chloroplasts was performed at 4°C for 5 min in the dark, import was carried out for 10 min at 25°C in light. For import analysis equal amounts of chloroplasts on a chlorophyll basis were used for SDS-PAGE. As control served the *in vitro* translation product of pCR*par4*. The [<sup>35</sup>S]methionine and -cysteine labeled translation, prebinding and import products were detected by autoradiography. For immunological detection of the mature *par* homolog in different pea chloroplast fractions the chloroplasts were treated according to the protocol described in [40] and stroma, thylakoid and envelope protein was an-

alyzed by SDS-PAGE and Western-blotting as described above.

### 3. Results

#### 3.1. Clone CR*par4* – an APS reductase homolog from *Catharanthus roseus*

A cDNA library constructed from *C. roseus* cell cultures that were starved for sulfate for 3 days before extraction of the mRNA was screened by phenotypic complementation of *cys* mutants from *E. coli*. A cDNA clone complementing the mutant *cysH* (*E. coli* JM96 FAK) which lacks PAPS reductase activity was isolated and further investigated to elucidate distinctive biochemical properties of its gene product. Clone CR*par4* consisted of 1775 bp with an open reading frame of 1392 bp. It encoded for a protein of 463 amino acid residues corresponding to a molecular mass of 51394 with a theoretical isoelectric point of 5.95. Over the entire length, the

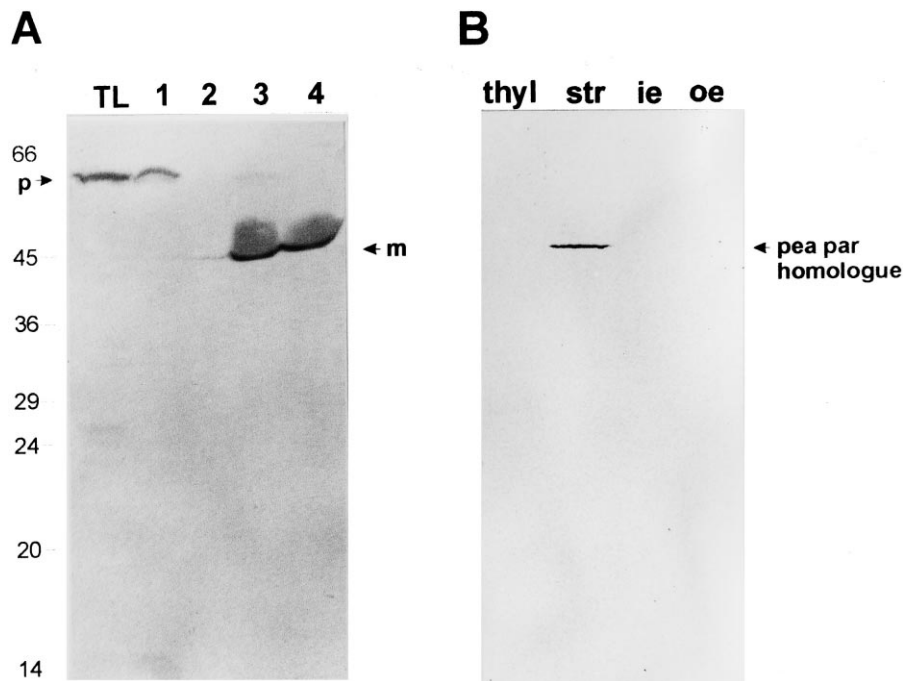


Fig. 3. Chloroplast localization of plant APS reductase. (A) Autoradiograph showing the in vitro translated, [ $^{35}$ S]methionine and -cysteine labeled precursor and the imported and processed CR $par4$  gene product separated by SDS-PAGE. In vitro translation, chloroplast import and import analysis by SDS-PAGE were performed as described in Section 2. Lanes: TL, in vitro translation product of pCR $par4$  (p=precursor); 1, prebinding of CR $par4$  precursor protein to chloroplasts; 2, prebinding of CR $par4$  precursor protein to chloroplasts and thermolysin treatment; 3, imported mature par gene product (m); 4, imported mature par gene product after thermolysin treatment of chloroplasts. (B) Immunodetection of a mature par homologue in pea chloroplast stroma by Western blotting of different pea chloroplast fractions prepared according to [40]. The mature pea par homologue was detected using anti-par $\Delta 1$  antibodies. thyl, thylakoid fraction; str, stroma fraction; ie, inner envelope fraction; oe, outer envelope fraction.

polypeptide was 73–76% identical to the APS reductases from *Arabidopsis thaliana* [1,2]. Like its homologs from *A. thaliana* the *C. roseus* protein consists of three different domains: a transit polypeptide with the putative function to direct the gene product into the plastid, a central PAPS reductase-like core, and a C-terminal extension with a putative redox-active cysteine disulfide center homologous to the thioredoxin-like domain of protein disulfide isomerase (pdi), hitherto designated as the thioredoxin-like pdi domain. The N-terminus of 71 residues is characterized by a high content of hydrophilic amino acids (11 serine and 3 threonine residues out of 71) which is indicative of a transit peptide for plastids. From residue 72 to 327 the core protein is 28% identical to the *cysH* PAPS reductase from *E. coli* [18], 33–35% identical to the PAPS reductase homolog *cysH1* from *Bacillus subtilis* [41] and 52% identical to *cysH* homolog from *Pseudomonas aeruginosa* (O0527). The alignment (Fig. 1) compares the full

length protein encoded by CR $par4$  with the primary structure of the homologous polypeptides from *A. thaliana* [1], *E. coli* [18] and *B. subtilis* [41]. The C-terminal extension of 136 amino acid residues shares 32% identity with the thioredoxin-like domain of protein disulfide isomerase from chicken and mouse [42,43].

### 3.2. Primary structure of the par $\Delta$ gene products

In order to analyze the catalytic properties of the individual domains of the gene product encoded by CR $par4$  we constructed two deletion clones using the pET16b vector system and expressed the corresponding his $_{10}$ -tag fusion proteins. The first protein lacked the putative transit peptide (designated 'par $\Delta 1$ '), the second (designated 'par $\Delta 2$ ') lacked the transit peptide and the thioredoxin-like pdi domain. The par $\Delta 1$  polypeptide consists of 433 amino acid residues with a mass of 48464. Par $\Delta 2$  consists of 292 residues with a

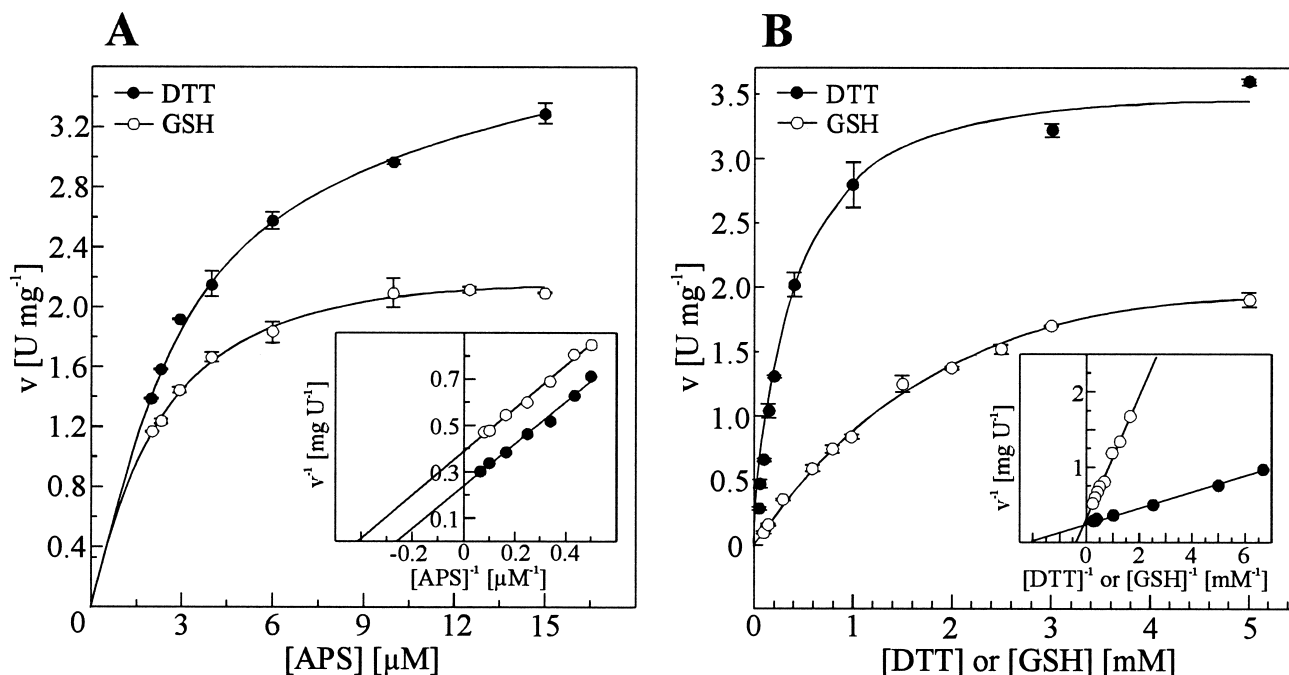


Fig. 4. Initial velocity kinetics of the recombinant par $\Delta$ 1 protein. (A) Michaelis–Menten plot of  $v$  versus [APS] at saturating concentrations of DTT (20 mM) (●) or GSH (20 mM) (○). Inset: Corresponding Lineweaver–Burk plot of  $v^{-1}$  versus [APS] $^{-1}$  to determine  $V_{\max}$  and  $K_m$  for APS. (B) Michaelis–Menten plot of  $v$  versus [DTT] (●) or [GSH] (○) at saturating APS concentrations (15  $\mu$ M). Inset: Lineweaver–Burk plot of  $v^{-1}$  versus [DTT] $^{-1}$  or [GSH] $^{-1}$  considering only the higher DTT and GSH concentrations to determine  $K_m$  for DTT and GSH. Velocity of sulfite formation was measured at 25°C in a reaction mixture containing 10 ng of purified par $\Delta$ 1 protein, 100 mM Tris-HCl pH 8.0, 10 mM Na<sub>2</sub>SO<sub>3</sub>, 0.5 M Na<sub>2</sub>SO<sub>4</sub>, 2–15  $\mu$ M [<sup>35</sup>S]APS, 50  $\mu$ M to 5 mM DTT or 50  $\mu$ M to 5 mM GSH. One unit is defined as the formation of 1  $\mu$ mol sulfite per min.

mass of 32898. The proteins expressed in *E. coli* were purified by affinity chromatography (Fig. 2). In the SDS-PAGE, under denaturing conditions both homogeneous his<sub>10</sub>-tag fusion proteins migrated to a position indicative of a considerably higher molecular weight than expected from its deduced molecular mass. Par $\Delta$ 1 travelled to a position corresponding to 58 kDa and par $\Delta$ 2 was found at a position corresponding to 43 kDa. Par $\Delta$ 1 was also used to raise polyclonal antibodies which were found monospecific for both products par $\Delta$ 1 and par $\Delta$ 2 (Fig. 2B). Degradation of the gene products is excluded as both immunoblots gave well defined single line precipitates. Antibodies against *E. coli* PAPS reductase did not cross-react with either par $\Delta$ 1 or par $\Delta$ 2 and vice versa anti:par $\Delta$ 1 did not react with PAPS reductase from *E. coli*, indicating that the immunological detection of recombinant par protein is not obscured by a background caused by the host.

### 3.3. Chloroplast import, processing in vitro and immunodetection

Import into the plastid was studied using the CRpar precursor protein. Plasmid pCRpar4 was linearized with endonuclease *Xho*I, transcribed and translated in vitro in a coupled assay using [<sup>35</sup>S]methionine and [<sup>35</sup>S]cysteine as described in Section 2. The precursor of approximately 58 kDa (Fig. 3A, lanes TL and 1) was imported into intact pea chloroplasts. It was processed to give a final product of approximately 45 kDa (Fig. 3A, lanes 3 and 4) which agrees well with the expected value for a processed par gene product of 44 kDa. In addition, we could detect a par homologous protein in the stroma fraction of pea chloroplasts using anti:par $\Delta$ 1 antibodies (Fig. 3B). Thylakoids, inner or outer envelope did not show any immunoreactive response. The detected pea protein had a size comparable to the processed par gene product as detected in the in vitro import assay.

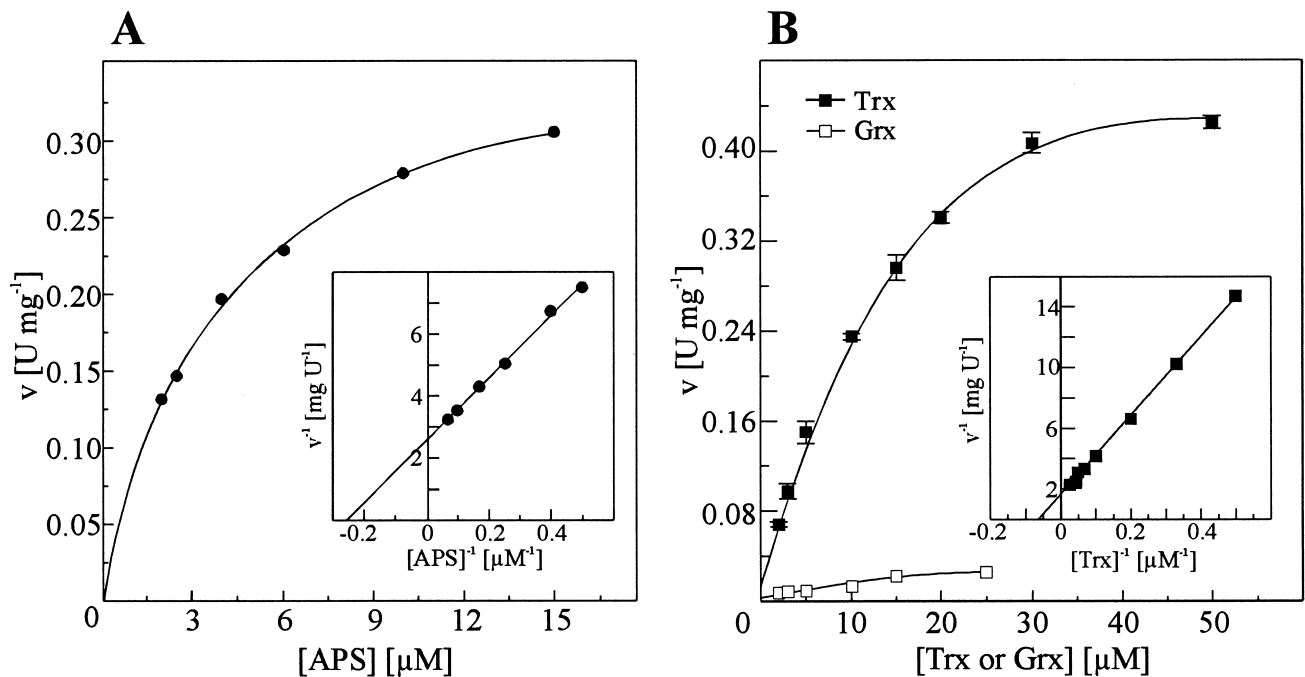


Fig. 5. Sulfite formation by the recombinant parΔ2 protein. (A) Michaelis–Menten plot of  $v$  versus [APS] at saturating concentrations of *E. coli* thioredoxin-1 (35 μM). Inset: Lineweaver–Burk plot of  $v^{-1}$  versus  $[APS]^{-1}$  to determine  $K_m$  and  $V_{max}$  for APS. (B) Michaelis–Menten plot of  $v$  versus [Trx] (■) and [Grx] (□) at saturating concentrations of APS (15 μM). Inset: corresponding Lineweaver–Burk plot of  $v^{-1}$  versus  $[Trx]^{-1}$  to determine  $K_m$  and  $V_{max}$  for *E. coli* thioredoxin-1. Velocity of sulfite formation was measured at 25°C applying 50 ng of purified parΔ2 protein, 100 mM Tris/HCl pH 8.0, 10 mM Na<sub>2</sub>SO<sub>3</sub>, 0.5 M Na<sub>2</sub>SO<sub>4</sub>, 2–15 μM [<sup>35</sup>S]APS, 2–50 μM *E. coli* thioredoxin-1 kept reduced by 10 mM DTT or 2–25 μM *E. coli* glutaredoxin-1 kept reduced by 10 mM GSH. One unit is defined as the formation of 1 μmol sulfite per min.

### 3.4. Kinetic properties of CRpar4 product, parΔ1 and parΔ2

Reaction conditions for APS reducing activity were optimized for parΔ1 and applied also to parΔ2. The reaction showed a  $Q_{10}$  of  $\approx 1.85$  (from 15–30°C) where the formation of sulfite was strictly linear when the enzyme concentration was kept from 10 to 1000 ng ml<sup>-1</sup>. The reaction time was kept  $\leq 180$  sec in order to convert less than 10% of the substrate APS to sulfite. A well defined pH optimum was obtained at pH 8.8. Unlike thioredoxin-dependent PAPS reductase from *E. coli*, sulfite formation with parΔ1 and parΔ2 is enhanced by high concentrations of anions that promote hydrophobic interactions between the reactants. Sulfate was more effective than chloride giving an optimal concentration between 0.35–0.5 M (data not shown). The CRpar4 (data not shown) and parΔ1 gene products used the monothiol glutathione or artificial reductants-like dithiothreitol and dithioerythritol as reductant, additional

thioredoxin was not required for sulfite formation. However, parΔ2 which is devoid of the C-terminal thioredoxin-like protein disulfide isomerase (pdi) domain was only active when supplemented with thioredoxin. In vitro, recombinant CRpar4 (data not shown), parΔ1, and parΔ2 were specific for APS as substrate. The same specificity for APS was previously reported for the APS reductases from *A. thaliana* [1,2]. The steady-state constants were determined from at least three independent experiments using enzyme from one preparation and are given with standard deviation.  $V_{max}$  for parΔ1 with APS as substrate and DTT as artificial reductant was  $4.2 \pm 0.6$  U mg<sup>-1</sup>. This corresponds to a molecular activity of 204 min<sup>-1</sup>. The affinity for APS in the artificial DTT system was  $3.8 \pm 0.9$  μM (Fig. 4A). When DTT was replaced by reduced glutathione a  $V_{max}$  of  $2.6 \pm 0.14$  U mg<sup>-1</sup> (turnover number, 126 min<sup>-1</sup>) was obtained while  $K_m$  APS  $2.5 \pm 0.23$  μM remained virtually unaffected. The true physiological reductants of the plant APS reductase are not yet known

and remain to be established. Since chloroplasts contain large amounts of reduced glutathione [44] and APS reductase is imported into the stroma, glutathione may be considered as possible reductant. The  $K_m$  of par $\Delta$ 1 for reduced glutathione was  $3 \pm 0.64$  mM with  $V_{max}$  of  $3.5 \pm 0.57$  U  $mg^{-1}$ . With DTT as reductant a  $K_m$  DTT of 0.4 mM and a  $V_{max}$  of 3.9 U  $mg^{-1}$  was obtained (Fig. 4B).

When the C-terminal thioredoxin-like pdi domain was deleted as in par $\Delta$ 2 the capability to reduce APS with DTT as reductant was lost, but activity could be restored by addition of exogenous thioredoxin. Thioredoxin could not be replaced by either DTT or GSH alone or glutaredoxin in combination with GSH. The affinity for thioredoxin was  $15.3 \pm 1.27$   $\mu$ M at saturating concentrations of APS (Fig. 5B).  $V_{max}$  of par $\Delta$ 2 was lowered to  $0.6 \pm 0.014$  U  $mg^{-1}$  while  $K_m$  APS with 3.8  $\mu$ M was not altered (Fig. 5A). The molecular activity of par $\Delta$ 2 was 20  $min^{-1}$  using *E. coli* thioredoxin.

The APS reductase contains eight cysteinyl residues. As yet, it is unclear whether these cysteinyl residues are involved in structural or regulatory functions. The effect of DTT as thiol reductant on the enzyme structure is seen in the SDS-PAGE under denaturing conditions. The concentrations of DTT used to establish the  $K_m$  APS value were high enough to monomerize the protein. However, in the absence of a strong disulfide reductant-like DTT, par $\Delta$ 1 had formed aggregates (Fig. 6) which could not be resolved by SDS. When 20 mM glutathione is used as reductant in the SDS-PAGE of par $\Delta$ 1 the monomer was found as with DTT. Yet, as APS reducing activity of par $\Delta$ 1 is even stable in 20 mM GSH or DTT for 30 min at 25°C (data not shown) it may be assumed that the reaction is catalyzed by a protein monomer, however, not excluding the possibility of a transient charge transfer complex in a homodimer.

The C-terminal extension of *C. roseus* APS reductase is described here as the thioredoxin-like pdi domain because of its YAPWCRFC motif that strongly resembles the YAPWCGHC cluster of the large family of protein disulfide isomerases [45]. The motif is also conserved in the *A. thaliana* proteins where the arginine residue is replaced by a proline. Disulfide isomerase activity of the par $\Delta$ 1 protein from *C. roseus* was measured as capacity to refold denatured RNase A. Denatured, reduced RNase A was rena-

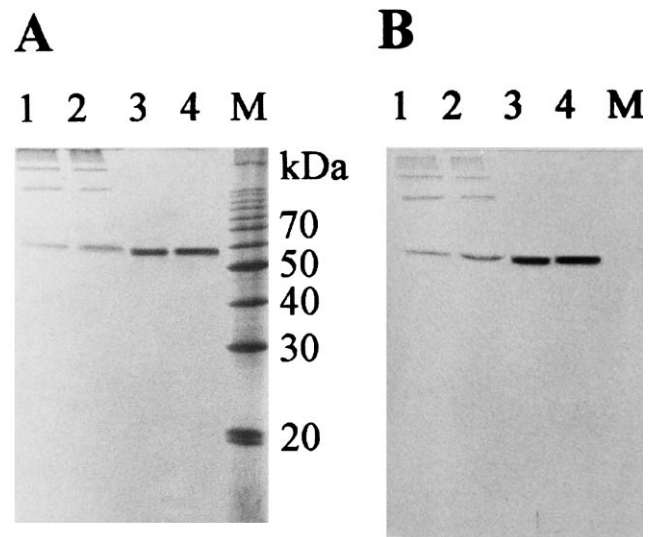


Fig. 6. Monomerization of the recombinant par $\Delta$ 1 protein by DTT. (A) SDS-PAGE of the purified par $\Delta$ 1 protein (2  $\mu$ g/lane) (12.5%, Coomassie blue staining) and (B) Western blot of A. Electrophoresis was done according to [28] using different concentrations of SDS and DTT as reductant in the samples. Lanes: 1, 1% (w/v) SDS, no reductant; 2, 2% (w/v) SDS, no reductant; 3, 1% (w/v) SDS and 6.7 mM DTT; 4, 2% (w/v) SDS and 6.7 mM DTT; M, molecular weight marker (10 kDa ladder, MBI Fermentas). Recombinant par $\Delta$ 1 protein was detected using anti-par $\Delta$ 1 antibodies.

tured by par $\Delta$ 1 to full activity within 70 min. Under identical conditions, PAPS reductase from *E. coli*, even at 10  $\mu$ M, reactivated only 15% of RNase A (Fig. 7).

The aspect of a thioredoxin-like function of the C-terminal extension was already mentioned for the enzymes from *A. thaliana* [1,2]. The property of thioredoxins to preferentially react as disulfide reductase rather than isomerase was analyzed for par $\Delta$ 1 and par $\Delta$ 2 using the insulin reductase assay [34]. Except for a slightly longer lag-phase, both proteins reduced insulin at a rate that was comparable to the rate<sup>3</sup> obtained with thioredoxin from *E. coli*. Not only par $\Delta$ 1 (35.4%) as expected, but also par $\Delta$ 2 (21.8%) showed a considerable disulfide reductase activity (Fig. 8). It is noteworthy that a disulfide reductase activity is also associated with the core protein of APS reductase and not only resident in the C-terminal thioredoxin-like pdi domain as previ-

<sup>3</sup> 100% with thioredoxin was  $\Delta A$  0.197  $min^{-1} \mu mol^{-1}$ .

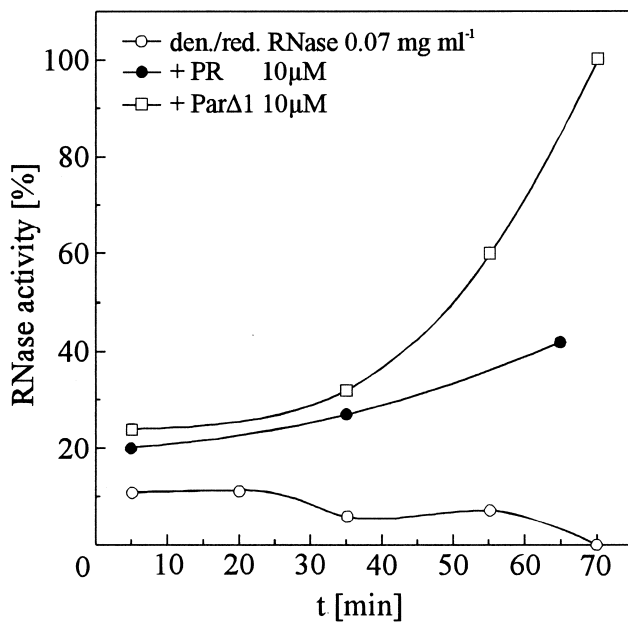


Fig. 7. Kinetic of the reactivation of denatured, reduced RNase by par $\Delta$ 1 protein. Reactivation of denatured (den.), reduced (red.) RNase ( $0.07 \text{ mg ml}^{-1}$ ) was tested in redox buffer alone ( $\circ$ ) ( $0.2 \text{ mM DTT}$ ,  $0.3 \text{ mM GSSG}$ ,  $3.3 \text{ mM MgCl}_2$ ,  $15 \text{ mM Tris/acetate pH 8.0}$ ) and in the presence of  $10 \text{ }\mu\text{M}$  par $\Delta$ 1-protein ( $\square$ ) or  $10 \text{ }\mu\text{M}$  *E. coli* PAPS reductase (PR) ( $\bullet$ ). RNase activity was measured in appropriate intervals as described in [36] and calculated relative to an equivalent amount of native RNase A.

ously suggested. It is pertinent to state that in addition to the redox-active YAPWCRFC<sub>386</sub> cluster in the C-terminal domain of the APS reductase a CXXC is also found further upstream in the core protein at SIGCEPC<sub>292</sub>.

As investigated by absorption spectroscopy, the recombinant plant-type APS reductase from *C. roseus* was isolated as a colorless protein that was devoid of chromophores, such as flavins or iron–sul-

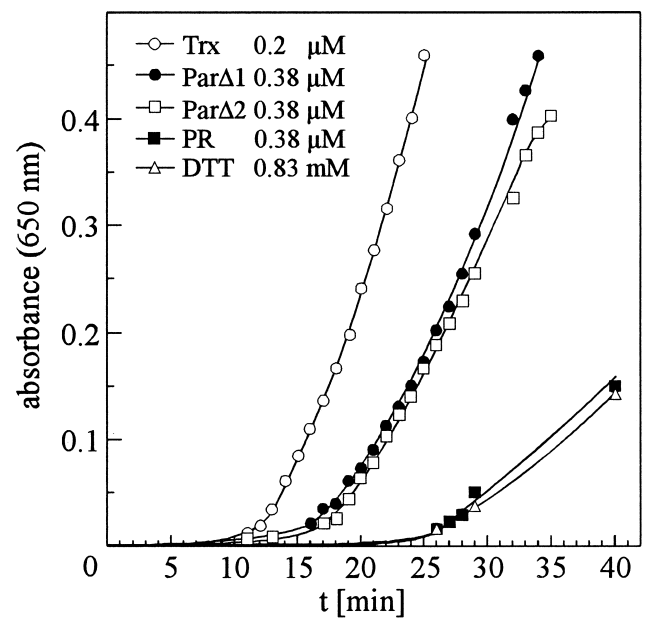


Fig. 8. Kinetics of DTT-dependent insulin reduction by par gene products. The incubation mixture contained in a final volume of  $600 \text{ }\mu\text{l}$   $83 \text{ mM}$  potassium phosphate pH 7.0,  $1.7 \text{ mM}$  EDTA,  $140 \text{ }\mu\text{M}$  bovine insulin,  $0.83 \text{ mM}$  DTT and  $0.38 \text{ }\mu\text{M}$  par $\Delta$ 1 protein ( $\bullet$ ) or  $0.38 \text{ }\mu\text{M}$  par $\Delta$ 2 protein ( $\square$ ). As positive control par proteins were replaced by  $0.2 \text{ }\mu\text{M}$  thioredoxin from *E. coli* ( $\circ$ ). As negative control served the non-enzymatical reduction of insulin by DTT ( $\triangle$ ). Further on  $0.38 \text{ }\mu\text{M}$  *E. coli* PAPS reductase (PR) was tested as catalyst ( $\blacksquare$ ).

fur clusters. In accordance with this finding, it did not display diaphorase activity with NADH as reductant and DCPIP as acceptor.

#### 4. Discussion

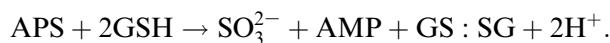
The *Catharanthus* CRpar4 cDNA encodes for a plant-type APS reductase that consists of a N-termi-

Table 1

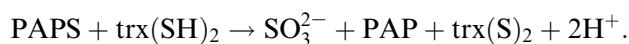
Structural and functional important amino acids in *E. coli* PAPS reductase [7] and their homologs in *B. subtilis* PAPS reductase [41], *C. roseus* APS reductase, and *A. thaliana* APS reductases [1,2]

Function	Motifs			
	<i>E. coli</i>	<i>B. subtilis</i>	<i>C. roseus</i>	<i>A. thaliana</i>
Substrate binding	SFG <sub>55</sub>	SFG	FSG	FSG
Purine ring orientation	DTG <sub>80</sub>	DTG	DTG	DTG
Kinked helix 7	K <sub>136</sub> –P <sub>139</sub>	K–P	K–P	K–P
Flexible lid	G <sub>155</sub> –RR <sub>158</sub> ...R <sub>164</sub>	G–RR...R	G–RK...R	G–RK...R
Dimer hinge	GY <sub>209</sub>	GY	GY	GY
Catalytic center thiolate	ECGLH <sub>242</sub>	ECGLH	ECGLH	ECGLH

nal transit peptide of 71 residues, a PAPS reductase-like core protein (residues 72–321), extended at its C-terminus by a thioredoxin-like protein disulfide isomerase domain (residues 321–463). In its primary structure, it is about 70% identical to APS reductases that have previously been described from *A. thaliana* [1,2]. In these first reports, it was shown that the *A. thaliana* proteins were specific for APS as substrate. Therefore it may be innocuous to state that the products of this reaction are sulfite and AMP as long as glutathione as reductant thiol can be kept in the reduced state:



In their first analysis of the *in vitro* properties, the authors suggested that the CXXC motif of the C-terminal extension could function as an intramolecular thioredoxin that transfers electrons from a thiol substrate to the reaction center of the APS reductase. GSH as electron donor would, however, imply that the APS reductase forms an enzyme–glutathione mixed disulfide with a cysteine of the CXXC site, before, in a second step, the enzyme gets fully reduced by a second GSH with the release of GS:SG. One of the intriguing questions about the mechanism of this enzyme is how sulfite can be released from APS without reacting with the product GS:SG. We started to investigate the function of the individual domains aiming for a deeper understanding of the reductive mechanism compared to the reaction catalyzed by microbial PAPS reductases [6]:



The recombinant plant APS reductase did not require thioredoxin and reduced PAPS *in vitro* only at a  $\approx 10^3$  lower rate than APS. The  $K_m$  values obtained for APS were in the micromolar range (2.5  $\mu\text{M}$ ). Using glutathione as reductant a  $V_{\text{max}}$  of 2.6  $\text{U mg}^{-1}$  was obtained resulting in a turnover number of 126  $\text{min}^{-1}$ . Par $\Delta 2$  lacking the C-terminal thioredoxin-like pdi domain only reduced APS when supplemented with exogenous thioredoxin.  $K_m$  for APS (3.8  $\mu\text{M}$ ) in this reconstituted system was in the same range whereas the molecular activity decreased to 20  $\text{min}^{-1}$ . These data strongly support the view that the catalytic function of the enzyme is located

in the core protein which is homologous to the bacterial PAPS reductases.

From the crystal structure of the *E. coli* enzyme [7] it is known that the protein folds into a central six-stranded  $\beta$ -sheet surrounded by nine  $\alpha$ -helices. The catalytic cleft is buried inside with a high positive surface potential that is proposed to direct the negatively charged substrate into its binding pocket. PAPS and APS reductases alike have identical and fully conserved residues in their primary structure which are known to contribute to the substrate binding site and to functional and structural elements in PAPS reductase (Table 1). In addition to the ECGLH motif that represents the catalytically indispensable cysteine thiolate redox center in the *E. coli* PAPS reductase [6], the residues DTG and SFG/FSG that form the modified PP-motif [46] are present as well as the R cluster in the flexible loop that covers the catalytic site. Including its C-terminal extension, APS reductase contains eight cysteine residues of which four are grouped in two CXXC motifs. A CC cluster is located at position 197/198, a single cysteine is found at position 308 of the polypeptide and in the ECGLH cluster. Of the two CXXC motifs, the C-terminal cysteine tetrapeptide YAPW-CRFC resembles most strongly the active site of a protein disulfide isomerase YAPWCGHCK [45] though glycine is replaced by arginine and histidine by phenylalanine. In the corresponding CPFC tetrapeptide from *A. thaliana* a proline is found instead of the glycine/arginine. The N-terminal CXXC motif of the APS reductase, the SIGCEPC<sub>292</sub> cluster, is identical with a motif found in the *cysH* homologs from *B. subtilis* and *P. aeruginosa*, indicating a closer relationship of these proteins when compared to the enterobacterial, fungal or cyanobacterial enzymes.

As shown for PAPS reductase and GMP synthetase [7] proteins of low identity in their primary still can show a similar secondary and tertiary structure. The secondary structure predicted for the CRpar4 protein according to Rost and Sanders [47–49] (PHDsec par4) is virtually identical to the secondary structure of the *E. coli* PAPS reductase (Fig. 1) deduced from the 3-D structure (DSSP 1sur). Length and position of those  $\alpha$ -helices and  $\beta$ -sheets are in good agreement with the *E. coli* enzyme which contribute to the nucleotide binding fold, including the purine binding PP motif (SFG<sub>55</sub>) and the DT motifs

(DTG<sub>80</sub>) interacting with the purine ring [7,46]. However, the prediction for plant APS reductase is unreliable from K<sub>184</sub> to P<sub>233</sub>. It seems noticeable that, except for the same region, the algorithm predicts the secondary structure elements in *E. coli* PAPS reductase with a high reliability as seen in the 3-D structure. In toto, this finding strongly supports the view that the nucleotide binding in PAPS and APS reductase is composed of highly similar secondary structural elements.

Three-dimensional structure identity provides valuable additional information in the question of possible functions. From structure prediction (using WHATIF [50]) it can be expected that with the exception of an extension of the loop connecting  $\beta$ 5– $\beta$ 6, but including the CC<sub>198</sub> and the SIGCEPC<sub>292</sub> motif, the plant core protein has a structure that is almost identical with the bacterial PAPS reductase of the *E. coli* type. This SIGCEPC cluster adjacent to the GY motif would be located on the outer rim of the catalytic cleft with the thiol groups pointing towards the catalytic cleft. By site-specific mutagenesis it was shown that the tyrosine (GY) residue is essential for the PAPS reductase reaction [6]. It remains to be shown by mutagenesis if the CXXC cluster in SIGCEPC motif assists in the transfer of electrons to the substrate.

As par $\Delta$ 2 APS reductase was inactive using GSH or DTT as reductant, the C-terminal domain of APS reductase is involved in electron transfer from GSH/DTT to APS. This C-terminal domain of the APS reductase with its YAPWCRFCK cluster has been described as thioredoxin-like [51], but also, more recently, as glutaredoxin [52]. Wray et al. could show that *E. coli* NADPH:trx reductase can be used to transfer electrons from NADPH to APS reductase suggesting that the C-terminal domain is capable of participating in the APS reductase reaction mechanism [51]. Nevertheless this experiment did not disclose which of the CXXC motifs interacted with the trx reductase. We have seen that par $\Delta$ 2 lacking the C-terminal thioredoxin-like pdi domain still reduces APS when supplied with exogenous thioredoxin. In this role thioredoxin cannot be replaced by glutaredoxin. The failure of glutaredoxin to serve as reductant of par $\Delta$ 2 is noteworthy as grx1 could replace trx1 as electron donor of the *E. coli* PAPS reductase ([53], Lillig et al. (in preparation)). Glutathione is a

useful reductant for the wild-type APS reductase implying that the native electron acceptor has properties of a glutaredoxin redox center. Its failure to serve as reductant may, however, also indicate that the electrons from glutathione can only enter via the C-terminal YAPWCRFC cluster whereas electrons provided to par $\Delta$ 2 by thioredoxin can be transferred directly to the reaction center as in the bacterial PAPS reductase or enter via the SIGCEPC cysteine cluster in the core protein. In this context, it remains most remarkable that the C-terminal deleted par $\Delta$ 2 APS reductase was still active as insulin reductase.

Up to this date, only recombinant APS reductases have been investigated. In the discussion of possible *in vivo* functions, it should be kept in mind that the protein with its high content of cysteines was expressed in an organism that is not capable of correct disulfide bond formation. This deficit could have led to a structure that is misfolded and, as consequence, lacks prosthetic groups or cofactors, which require the native structure for insertion. Hence, a native plant product may well have properties that are not yet recognized.

Moreover, APS reductase was tested *in vitro* with APS as substrate. Until today, the question of the *in vivo* steady-state concentration of APS is unanswered. APS kinase [54,55] is also located in the chloroplastlike plant APS reductase and competes for APS as substrate. However, plant APS kinase is a very efficient enzyme with high affinity for both substrates ( $K_m$  ATP 14.3  $\mu$ M,  $K_m$  APS  $\leq$  0.28  $\mu$ M) and a high turnover [32,56]. It is activated by thiolslike the enzyme from *Chlamydomonas reinhardtii* [57] and it forms a phosphorylated enzyme intermediate like its counterpart from *E. coli* [58]. If APS is used as physiological substrate also by APS reductase, the high efficiency of APS kinase would severely impair the flow of sulfur into cysteine. Future work will show how the activities of APS reductase and APS kinase can operate in the same compartment as both appear to be fully active under identical conditions.

### Acknowledgements

We wish to thank Prof. E.W. Weiler (Plant Physiology, Bochum) for providing the *C. roseus* cell cul-

tures. Glutaredoxin-1 was a kind gift of Dr. F. Aslund (Harvard University, USA). The financial support of the Deutsche Forschungsgemeinschaft, Bonn, is gratefully acknowledged.

## References

- [1] J.M. Gutierrez-Marcos, M.A. Roberts, E.I. Campbell, J.L. Wray, *Proc. Natl. Acad. Sci. USA* 93 (1996) 13377–13382.
- [2] A. Setya, M. Murillo, T. Leustek, *Proc. Natl. Acad. Sci. USA* 93 (1996) 13383–13388.
- [3] A. Schmidt, *Arch. Microbiol.* 93 (1973) 29–52.
- [4] W.A. Abrams, J.A. Schiff, *Arch. Microbiol.* 94 (1973) 1–10.
- [5] J.D. Schwenn, *Z. Naturforsch.* 44c (1989) 504–508.
- [6] U. Berendt, T. Haverkamp, A. Prior, J.D. Schwenn, *Eur. J. Biochem.* 233 (1995) 347–356.
- [7] H. Savage, G. Montoya, C. Svensson, J.D. Schwenn, *I. Sinning, Structure* 5 (1997) 895–906.
- [8] A. Schmidt, K. Jäger, *Ann. Rev. Plant Physiol. Plant Mol. Biol.* 43 (1992) 325–349.
- [9] T. Leustek, *Physiol. Plantarum* 97 (1996) 411–419.
- [10] J.D. Schwenn, *Z. Naturforsch.* 49c (1994) 531–539.
- [11] J.D. Schwenn, in: J.W. Cram, L.J. de Kok, I. Stulen, C. Brunold, H. Rennenberg (Eds.) *Sulphur Metabolism in Higher Plants*, Backhuys, Leiden, 1997, pp. 39–58.
- [12] R. Hell, *Planta* 202 (1997) 138–148.
- [13] M.H. Zenk, H. El-Shagi, H. Arens, J. Stöckigt, E.W. Weiler, B. Deus, in: U. Barz, E. Reinhard, M.H. Zenk (Eds.) *Plant Tissue Culture and its Biotechnological Application*, Springer, Berlin, 1977, pp. 27–43.
- [14] J.D. Schwenn, H. El-Shagi, A. Kemena, E. Petrak, *Planta* 144 (1979) 419–425.
- [15] J.D. Schwenn, A. Kemena, *Planta* 160 (1984) 151–158.
- [16] J.D. Schwenn, U. Schriek, H.H. Kiltz, *Planta* 158 (1983) 540–549.
- [17] Y. Hatzfeld, N. Cathal, C. Grignon, J.C. Davidian, *Plant Physiol.* 116 (1998) 1307–1313.
- [18] F.A. Krone, G. Westphal, J.D. Schwenn, *Mol. Gen. Genet.* 225 (1991) 314–319.
- [19] F.W. Studier, B.A. Moffat, *J. Mol. Biol.* 189 (1986) 113–130.
- [20] H.J. Vogel, D.M. Bonner, *J. Biol. Chem.* 218 (1956) 97–106.
- [21] J. Sambrook, E.F. Fritsch, T. Maniatis, *Molecular Cloning. A Laboratory Manual*, Cold Spring Harbor Laboratory Press, Cold Spring Harbor, NY, 1989.
- [22] D. Hanahan, in: D.M. Glover (Ed.), *DNA Cloning*, Vol. I, 1985, pp. 109–135.
- [23] W.J. Dower, J.F. Miller, C.W. Ragsdale, *Nucleic Acids Res.* 16 (1988) 6127–6145.
- [24] E.M. Linsmaier, F. Skoog, *Physiol. Plant.* 18 (1965) 100–127.
- [25] P. Chomczynski, N. Sacchi, *Anal. Biochem.* 162 (1987) 156–159.
- [26] A. Vekris, *Nucleic Acids Res.* 22 (1994) 4842–4843.
- [27] M.M. Bradford, *Anal. Biochem.* 72 (1976) 669–670.
- [28] U.K. Laemmli, *Nature* 227 (1970) 680–685.
- [29] H. Towbin, T. Staehelin, J. Gordon, *Proc. Natl. Acad. Sci. USA* 76 (1979) 4350–4364.
- [30] J.D. Schwenn, U. Schriek, *Z. Naturforsch.* 42c (1987) 93–102.
- [31] U. Schriek, J.D. Schwenn, *Arch. Microbiol.* 145 (1986) 32–38.
- [32] S. Schiffmann, PhD. Thesis, 1998, Bochum.
- [33] J.D. Schwenn, H.G. Jender, *J. Chromatogr.* 193 (1980) 285–290.
- [34] A. Holmgren, *J. Biol. Chem.* 254 (1979) 9627–9632.
- [35] A. de Crouy-Chanel, M. Kohiyama, G. Richarme, *J. Biol. Chem.* 270 (1995) 22669–22672.
- [36] Y. Akiyama, S. Kamitani, N. Kusukuwa, K. Ito, *J. Biol. Chem.* 267 (1992) 22440–22445.
- [37] P. Blackburn, *J. Biol. Chem.* 254 (1979) 12484–12487.
- [38] E. Muckel, J. Soll, *J. Biol. Chem.* 271 (1996) 23846–23852.
- [39] K. Waegemann, J. Soll, *Plant J.* 1 (1991) 149–158.
- [40] J. Lübeck, L. Heins, J. Soll, *Physiol. Plant.* 100 (1997) 53–64.
- [41] M.C. Mansilla, D. de Mendoza, *J. Bacteriol.* 179 (1997) 976–981.
- [42] J.A. Bassuk, R.A. Berg, *J. Biol. Chem.* 266 (1991) 23732–23738.
- [43] Q.H. Gong, T. Fukuda, C. Parkison, S.Y. Cheng, *Nucleic Acids Res.* 16 (1988) 1203.
- [44] J.M. Williamson, A. Meister, *Proc. Natl. Acad. Sci. USA* 78 (1981) 936–939.
- [45] R.B. Freedman, T.R. Hirst, M.F. Tuite, *Trends Biochem. Sci.* 19 (1994) 331–336.
- [46] P. Bork, E.V. Koonin, *Proteins* 20 (1994) 347–355.
- [47] B. Rost, C. Sander, *J. Mol. Biol.* 232 (1993) 584–599.
- [48] B. Rost, C. Sander, P. Schneider, *Comput. Appl. Biosci.* 10 (1994) 53–60.
- [49] B. Rost, C. Sander, *Proteins* 19 (1994) 55–72.
- [50] G. Vriend, *J. Mol. Graph.* 8 (1990) 52–56.
- [51] J.L. Wray, E.I. Campbell, M.A. Roberts, J.F. Gutierrez-Marcos, *Chem. Biol. Interact.* 109 (1998) 153–167.
- [52] J.A. Bick, F. Aslund, Y. Chen, T. Leustek, *Proc. Natl. Acad. Sci. USA* 95 (1998) 8404–8409.
- [53] M.L.S. Tsang, *J. Bacteriol.* 146 (1981) 1059–1066.
- [54] H. Arz, G. Gisselmann, S. Schiffmann, J.D. Schwenn, *Biochim. Biophys. Acta* 1218 (1994) 447–452.
- [55] S. Schiffmann, J.D. Schwenn, *Plant Physiol.* 117 (1998) 1125.
- [56] S. Lee, T. Leustek, *Biochem. Biophys. Res. Commun.* 247 (1998) 171–175.
- [57] J.D. Schwenn, U. Schriek, *FEBS Lett.* 170 (1984) 76–80.
- [58] C. Satischandran, G.D. Markham, *J. Biol. Chem.* 264 (1989) 15012–15021.
- [59] W. Kabsch, C. Sander, *Biopolymers* 22 (1983) 2577–2637.